JACS
JOURNAL OF THE AMERICAN CHEMICAL SOCIETY
Communication
pubs.acs.org/JACS

Long-Range C−H Bond Activation by Rh^{III}-Carboxylates

Matthew E. O'Reilly,[†] Ross Fu,[‡] Robert J. Nielsen,[‡] Michal Sabat,[§] William A. Goddard, III,*[,‡] and T. Brent Gunnoe*[,†]

[†]Department of Chemistry, University of Virginia, Charlottesville, Virginia 22904-4319, United States
[‡]Materials and Process Simulation Center, California Institute of Technology, Pasadena, California 91125, United States
[§]Nanoscale Materials Characterization Facility, Department of Materials Science and Engineering, University of Virginia, Charlottesville, Virginia 22904-4319, United States

Supporting Information

ABSTRACT: Traditional C−H bond activation by a concerted metalation−deprotonation (CMD) mechanism involves precoordination of the C−H bond followed by deprotonation from an internal base. Reported herein is a "through-arene" activation of an uncoordinated benzylic C−H bond that is 6 bonds away from a Rh^{III} ion. The mechanism, which was investigated by experimental and DFT studies, proceeds through a dearomatized xylene intermediate. This intermediate was observed spectroscopically upon addition of a pyridine base to provide a thermodynamic trap.

The selective activation of C−H bonds by transition metal catalysts has garnered considerable attention as an important step for the functionalization of hydrocarbons.[1−5] Motivation to investigate this bond-breaking event stems from the search for more economical and atom-efficient routes to attain complex molecules over traditional cross-coupling reactions.[6−14] However, such applications are predicated on catalysts that can selectively activate the desired C−H bond. A common strategy for controlling selectivity is to use directing groups that bring the desired C−H bond within the metal coordination sphere.[15] While the majority of directing groups activate *ortho*-C−H bonds, significant advances have been made with new *meta*-selective directing groups.[16−18] In addition, new methodologies to control the selectivity of the C−H bond breaking event include steric directing groups,[19] removable templates,[20−25] and noncovalent supramolecular interactions.[26] A new thrust has been directed toward eliminating directing groups altogether.[27]

Complementing these advances, mechanistic and DFT studies have been central toward progressing the understanding of C−H bond activation. For Rh-based catalysts, several mechanisms for C−H activation have been described, which include metalloradical,[28−30] oxidative addition (OA),[14,31,32] electrophilic activation,[33] and internal electrophilic substitution (IES),[34,35] which is often related to concerted metalation−deprotonation (CMD).[12,14,31,32,36] To our knowledge, for all reported mechanisms the desired C−H bond is precoordinated to the metal prior to activation. We considered the possibility that the C−H bond may not need to be directly bound to the metal. Such a mechanism would offer new opportunities to redirect C−H bond activation to new sites. Herein, we show the potential of a variation of CMD for the activation of an uncoordinated C−H bond that is *6 bonds away from the metal center*.

In the CMD and IES mechanisms, a key ingredient is an electrophilic metal center that must polarize the C−H bond toward deprotonation. An exemplary case of a highly electrophilic Rh^{III} complex is the "$Rh(TFA)_3$" species {TFA = trifluoroacetate},[37,38] which has been shown to activate aromatic C−H bonds without directing groups for oxidative carbonylation of arenes.[33] Our approach was to confine the substrate in an unusual position near an electrophilic "$Rh^{III}(TFA)_3$" unit. Scheme 1 depicts the proposed ligand, a xylene-bridged diquinoline (Q_2X), which provides a xylene as an internal substrate near the coordination site of the reactive "$Rh^{III}(TFA)_3$" unit. Ligands having a similar design to Q_2X have been reported by Song and Wang.[39,40] More specifically, the unique steric interactions from such ligands during C−H bond activation of ethylbenzene by Pt(II)−Me complexes have been studied.[40]

Scheme 1. Synthesis of 8,8′-(4,5-*o*-Xylene)diquinoline (1), (Q_2X)Rh(TFA)(COE) (2), and (Q_2X)$Rh(TFA)_3$ (3)[a]

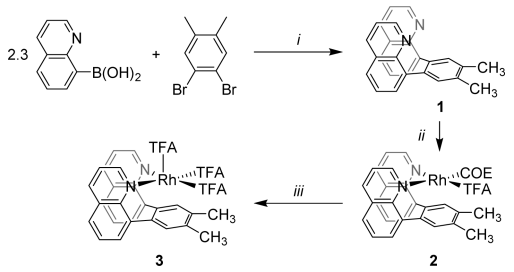

[a](*i*) 10% $Pd(PPh_3)_4$, 15 K_3PO_4, DMF/H_2O (1:1), 100−120 °C; (*ii*) 0.5 {$Rh(COE)_2(\mu$-TFA)$\}_2$, THF; (*iii*) ex. $Cu(TFA)_2$, HTFA.

The proposed ligand **1**, 8,8′-(4,5-*o*-xylene)diquinoline (Q_2X), was synthesized in a 38% isolated yield by a Pd-catalyzed Suzuki coupling (Scheme 1). The proligand **1** is C_s-symmetric with seven aromatic resonances appearing between 7.0 and 8.7 ppm with the *ortho*-protons adjacent to the N atom being the furthest downfield in the ^1H NMR spectrum. The methyl protons resonate at 2.20 ppm.

Treating **1** with {$Rh(COE)_2(\mu$-TFA)$\}_2$ {COE = cyclooctene} in THF provides (Q_2X)Rh(TFA)(COE) (**2**) as an orange

Received: August 14, 2014
Published: October 10, 2014

   dx.doi.org/10.1021/ja508367m | *J. Am. Chem. Soc.* 2014, 136, 14690−14693

powder after precipitation with hexanes (Scheme 1). The ^{1}H NMR spectrum of complex **2** contains two isomers in a 10:1 ratio. The major product contains 14 aromatic resonances that are consistent with the overall C_1-symmetry. A dramatic change in chemical shifts is experienced by one of the quinoline units. The *ortho*-proton of one quinoline unit appears at 10.6 ppm, while the other remains at 8.27 ppm.

Crystals of complex **2** suitable for X-ray diffraction were grown by slow evaporation of a concentrated CH_2Cl_2 solution, leading to the structure in Figure 1. As expected, the xylene fragment

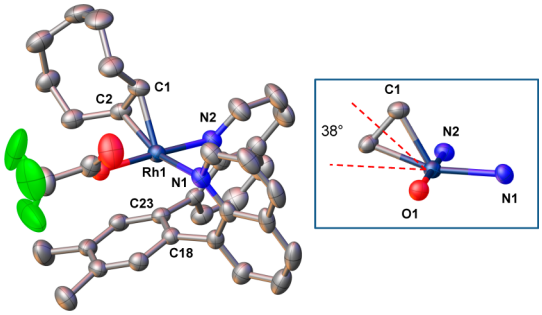

Figure 1. (Left) Single crystal X-ray structure of **2** (50% probability level). Calculated hydrogen and disorder positions for the $-CF_3$ group are removed for clarity. Selected bond lengths (Å): C23−Rh1 2.540(2), C18−Rh1 2.598(2), C1−Rh1 2.091(3), C2−Rh1 2.106(2). Selected bond angles (deg): N1−Rh1−C1 122.66(9), N1−Rh1−C2 162.10(9). (Right) Truncated depiction of the metal coordination sphere.

resides underneath the Rh^I coordination plane. More specifically, the rhodium atom sits above C23 and C18 atoms, but the Rh···C distances of 2.540(2) and 2.598(2) Å are too long to have a significant bonding interaction.[41−46] The xylene fragment makes a canopy covering the metal ion, but not interacting with it. This canopy cover causes steric interaction with the large cyclooctene (COE) ligand pushing the center of the coordinated COE ligand to lie 38° above the square plane formed by N1, N2, and O1 atoms (see inset of Figure 1).

Although there is some spectroscopic evidence to support a $Rh^{III}(TFA)_3$ fragment,[47] to our knowledge a complex possessing the $Rh^{III}(TFA)_3$ unit has never been isolated. Our initial attempt to synthesize $(Q_2X)Rh(TFA)_3$ (**3**) involved treating complex **2** with $Cu(TFA)_2$ in CH_2Cl_2 or THF and resulted in an unidentifiable purple mixture with no spectroscopic evidence for the formation of **3**. Changing the solvent to HTFA alters the outcome; the reaction proceeds cleanly yielding complex **3** in a 49% isolated yield (Scheme 1). While complex **3** is stable in $CHCl_3$ and CH_2Cl_2 at rt, it slowly decomposes in THF to an unidentifiable mixture that is purple. The ^{1}H NMR spectrum of **3** in $CDCl_3$ is consistent with a C_s-symmetric complex. The *ortho*-protons of the quinoline resonate at 9.28 ppm, and the methyl protons appear at 2.42 ppm. The ^{19}F NMR spectrum of **3** contains two TFA peaks at 74.9 and 75.0 ppm in a 2:1 ratio, respectively.

Attempts to isolate crystals of **3** suitable for X-ray crystallography were unsuccessful due to their small size and gradual decomposition, but DFT calculations provide insight into the structure of **3** (Figure 2). The Rh−O and Rh−N bond distances are calculated to be in the ranges of 2.01−2.03 Å and 2.10−2.14 Å, respectively, which is within the standard 2.00−2.15 Å bond length range. The canopy-type ligand places the Rh^{III} ion in a less stable 5-coordinate environment[48] with the xylene fragment at the vacant coordination site. The computed

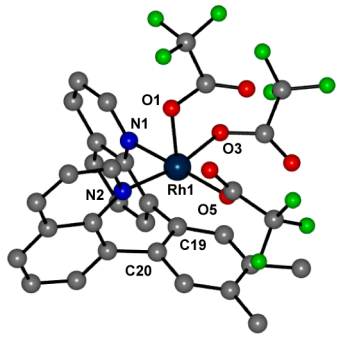

Figure 2. DFT optimized structure of complex **3**. Selected bond lengths (Å): C19−Rh1 2.50, C20−Rh1 2.66. Calculated hydrogen positions were removed for clarity.

C19 and C20 atoms are 2.50 and 2.66 Å away from the Rh atom, respectively, and still too far to have bonding interactions to the Rh metal center. From 1D and 2D NMR spectroscopy, there is no evidence to suggest a bonding interaction between the xylene π-bonds and the Rh^{III} metal center. For instance, the ^{13}C NMR displays modest downfield chemical shifts for C19 and C20 at 146.8 ppm from complex **2** (~136.0 ppm), and there is no evidence of $^1J_{Rh-C}$ coupling.

Heating **3** in DTFA at 90 °C for 2 h resulted in complete deuterium exchange with the xylene methyl protons forming **3**-d_6. A likely mechanism for this transformation involves a long-range intramolecular C−H bond activation to form a dearomatized xylene intermediate **3a** (Scheme 2). To accom-

Scheme 2. Proposed Mechanism of C−H Bond Activation from Complex 3 through Dearomatized Intermediate 3a during H/D Exchange with DTFA

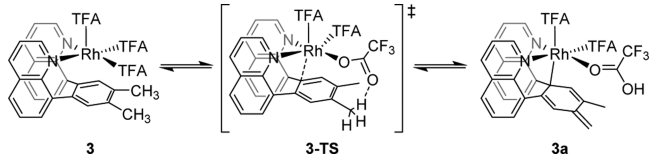

plish this feat, the methyl C−H bonds must be polarized by a Rh^{III} metal center that is 6 bonds away unless some intermolecular bimetallic process occurs. Monitoring the reaction by ^{1}H NMR spectroscopy reveals a first-order depletion of the H atoms on the methyl group (Figure 3), supporting the proposed intramolecular pathway. Analyzing the rate of H/D exchange at multiple temperatures between 70 and 100 °C

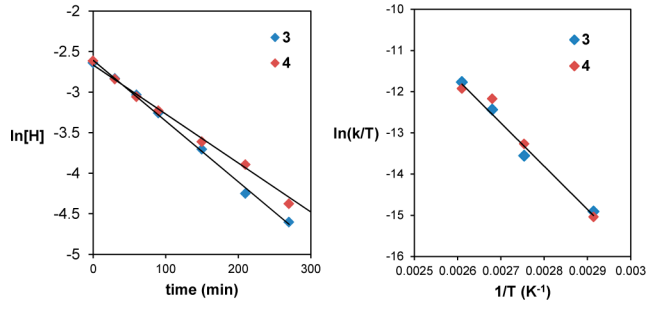

Figure 3. ln[H] vs time (left, 70 °C) {where [H] designates the methyl protons' concentration; e.g., initial [H] = 6 × [3]} and Eyring plots (right, 70−110 °C) for H/D exchange for complex **3** in HTFA and **4** in d_3-AcOD.

dx.doi.org/10.1021/ja508367m | J. Am. Chem. Soc. 2014, 136, 14690−14693

yielded $\Delta H^{\ddagger} = 21(2)$ kcal/mol and $\Delta S^{\ddagger} = -16(5)$ cal/mol·K for the C−H bond activation barrier.

DFT calculations were employed to corroborate the proposed mechanism. For the proposed transition state **3-TS** depicted in Scheme 2, the calculated activation energy of $\Delta H^{\ddagger}_{298} = 22.4$ kcal/mol and $\Delta S^{\ddagger}_{298} = -6.0$ cal/mol·K are remarkably close to the experimental values (see above). The experimental $\Delta S^{\ddagger}$ slightly exceeds computed values, which may be due to solvent rearrangement during the transition state. Figure 4 depicts the

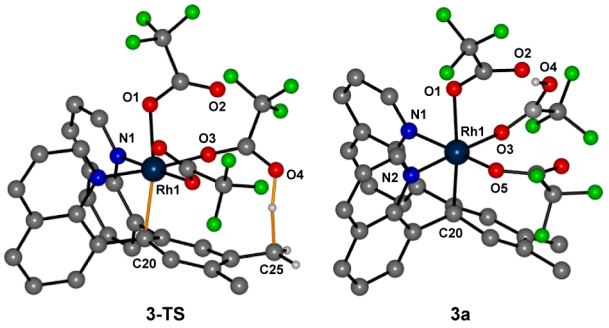

Figure 4. DFT optimized structure of transition state **3-TS** (left) and intermediate **3a** (right). Yellow bonds depict the intermediary bonds. Selected bond lengths of **3-TS** (Å): C20−Rh1 2.244, C25−H 1.441, O4−H 1.211; that of **3a** (Å): C20−Rh1 2.131. Calculated hydrogen positions except for the H25 (**3-TS**) and HTFA (**3a**) were removed for clarity.

DFT optimized structure of **3-TS** and the dearomatized intermediate **3a**, which provides insight into the structural changes during and after the C−H bond activation. Noticeably, the C20−Rh1 distance contracts to 2.244 Å during the transition state (**3-TS**), and the C25−H distance elongates from 1.09 Å (of **3**) to 1.44 Å, supporting concerted movement of metalation and deprotonation events. Meanwhile, the ring begins to dearomatize and bends down and away from the Rh^{III} coordination plane until a new Rh1−C20 bond (2.13 Å) of **3a** is formed. The free energy of the proposed intermediate **3a** is calculated to be 4.8 kcal/mol (298 K) above the starting complex **3**.

Next, we probed the influence of a different acidic medium on the rate of deuterium incorporation into the ligand's methyl groups. Dissolving complex **3** in d_3-AcOD displaces two

Scheme 3. In Situ Preparation of $(Q_2X)Rh(TFA)(d_3\text{-}OAc)_2$ (4)

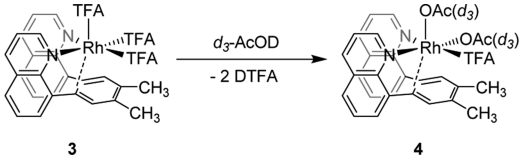

coordinated TFA groups to cleanly afford **4** (Scheme 3). The ^{1}H NMR spectrum of **4** contains 14 aromatic resonances and two methyl resonances at 2.45 and 2.32 ppm, consistent with the proposed C_1-symmetric species. DFT calculations confirm that this arrangement of the OAc ligands is the most stable isomer (Scheme S2). Additionally, the ^{19}F NMR spectrum contains a broad HTFA signal at −71.9 ppm and coordinated TFA (−70.3 ppm) in an approximate 2:1 ratio.

Heating complex **4** in d_3-AcOD resulted in a H/D exchange at the methyl position (Scheme 4). Monitoring the rate of H/D

Scheme 4. H/D Exchange from Complex 4 and Subsequent Conversion to $(Q_2X)Rh(d_3\text{-}OAc)_3$ (5)

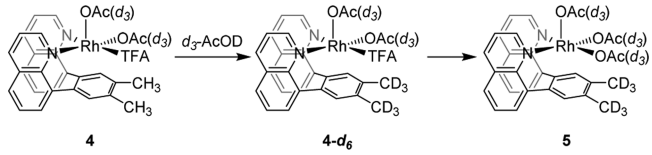

exchange yielded nearly identical ln[H] vs time and Eyring plots for H/D exchange as in the case for **3** (Figure 3). The new activation energy parameters for H/D exchange for **4** were determined to be $\Delta H^{\ddagger} = 21(2)$ kcal/mol and $\Delta S^{\ddagger} = -14(6)$ cal/mol·K, which are impressively similar to those of **3** in DTFA. Over the course of the reaction, complex **4** slowly displaces the last coordinated TFA to yield complex **5**. The conversion to **5** is three times slower than the methyl H/D exchange $\{k_{rel} = 3.0(3)\}$. Supporting the assignment of complex **5** is the overall C_s-symmetry in solution and 2D NMR characterization, but complex **5** could not be isolated from the acetic acid solvent.[49] In addition, the ^{19}F NMR spectrum contains only free HTFA at −70.3 ppm.

DFT calculations for the H/D exchange for **4** yielded two possible pathways (Scheme 5). The coordinated TFA could

Scheme 5. Two Possible H/D Exchange Transition States for Complex 4 Showing TFA Deprotonation (Left) and OAc Deprotonation (Right) Routes[a]

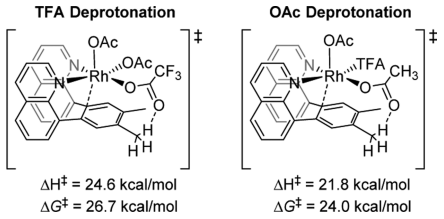

[a]DFT calculated $\Delta H^{\ddagger}$ and $\Delta G^{\ddagger}$ (298 K) associated with each transition state are presented underneath.

deprotonate the methyl group. The calculated $\Delta H^{\ddagger}_{298}$ was 24.6 kcal/mol, which is 2.2 kcal/mol higher than the calculated barrier for **3**. By the OAc partaking in the deprotonation event, the $\Delta H^{\ddagger}$ is lowered by 2.8 to 21.8 kcal/mol. The calculated entropy of activation remained constant for both the TFA and OAc pathways.

Central to the proposed mechanism of C−H bond dissociation by complex **3** is the dearomatized intermediate **3a** (Scheme 6). To verify this intermediate we added pyridine to **3**, which immediately deprotonated the methyl C−H bond to yield complex **6** *in situ*. The ^{1}H NMR spectrum of **6** reveals four new singlets at 6.49, 6.07, 5.63, and 5.26 ppm, consistent with the dearomatized ring, and the corresponding olefinic carbons appear at 110.7, 128.7, and 139.6 ppm. Slow decomposition of

Scheme 6. Deprotonation of 3 To Afford Complex 6

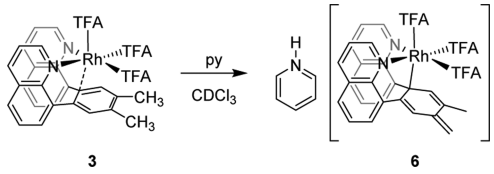

dx.doi.org/10.1021/ja508367m | J. Am. Chem. Soc. 2014, 136, 14690−14693

complex **6** over a course of 1 h at rt prevented isolation and further characterization.

In summary, we have demonstrated that the Rh center can reside over 4 Å away and yet still activate benzylic C−H bonds toward deprotonation by an internal base. Such a long-range intramolecular C−H bond activation, where an uncoordinated C−H bond becomes activated by a metal center that is 6 bonds away, is unprecedented. The mechanism proceeds through a dearomatized intermediate complex **3a** that results in Rh−C bond formation, which we were able to trap (complex **6**) upon the addition of pyridine. These results provide a new perspective on potential routes to C−H activation that may be helpful in designing catalysts with new selectivity. Additionally, it is possible that catalysts that activate benzylic C−H bonds may unknowingly proceed through a similar long-range mechanism.

■ ASSOCIATED CONTENT

Supporting Information

Experimental procedures, NMR spectra, DFT calculations, and single crystal X-ray structure. This material is available free of charge via the Internet at http://pubs.acs.org.

■ AUTHOR INFORMATION

Corresponding Authors

tbg7h@virginia.edu

wag@wag.caltech.edu

Notes

The authors declare no competing financial interest.

■ ACKNOWLEDGMENTS

The authors acknowledge support from the Center for Catalytic Hydrocarbon Functionalization, an Energy Frontier Research Center funded by the US Department of Energy, Office of Science, Office of Basic Energy Sciences under Award Number DE-SC0001298. We thank Thomas Rey for assistance with the single crystal X-ray diffraction experiments.

■ REFERENCES

(1) Webb, J. R.; Bolano, T.; Gunnoe, T. B. *ChemSusChem* **2011**, *4*, 37.

(2) Webb, J. R.; Burgess, S. A.; Cundari, T. R.; Gunnoe, T. B. *Dalton Trans.* **2013**, *42*, 16646.

(3) Hashiguchi, B. G.; Bischof, S. M.; Konnick, M. M.; Periana, R. A. *Acc. Chem. Res.* **2012**, *45*, 885.

(4) Stahl, S. S.; Labinger, J. A.; Bercaw, J. E. *Angew. Chem., Int. Ed.* **1998**, *37*, 2181.

(5) Goldberg, K. I.; Goldman, A. S. *Activation and Functionalization of C−H Bonds*; ACS Symposium Series 885; American Chemical Society: Distributed by Oxford University Press: Washington, DC, 2004; p 1.

(6) Yeung, C. S.; Dong, V. M. *Chem. Rev.* **2011**, *111*, 1215.

(7) Wencel-Delord, J.; Droge, T.; Liu, F.; Glorius, F. *Chem. Soc. Rev.* **2011**, *40*, 4740.

(8) Thansandote, P.; Lautens, M. *Chem.—Eur. J.* **2009**, *15*, 5874.

(9) Sun, C. L.; Li, B. J.; Shi, Z. J. *Chem. Rev.* **2011**, *111*, 1293.

(10) McGlacken, G. P.; Bateman, L. M. *Chem. Soc. Rev.* **2009**, *38*, 2447.

(11) Lyons, T. W.; Sanford, M. S. *Chem. Rev.* **2010**, *110*, 1147.

(12) Kuhl, N.; Hopkinson, M. N.; Glorius, F. *Angew. Chem., Int. Ed.* **2012**, *51*, 8230.

(13) Giri, R.; Shi, B. F.; Engle, K. M.; Maugel, N.; Yu, J. Q. *Chem. Soc. Rev.* **2009**, *38*, 3242.

(14) Colby, D. A.; Bergman, R. G.; Ellman, J. A. *Chem. Rev.* **2010**, *110*, 624.

(15) Cuesta, L.; Urriolabeitia, E. P. *C−H and C−X Bond Functionalization: Transition Metal Mediation*; The Royal Society of Chemistry: 2013; p 262.

(16) Duong, H. A.; Gilligan, R. E.; Cooke, M. L.; Phipps, R. J.; Gaunt, M. J. *Angew. Chem., Int. Ed.* **2011**, *50*, 463.

(17) Phipps, R. J.; Gaunt, M. J. *Science* **2009**, *323*, 1593.

(18) Leow, D.; Li, G.; Mei, T. S.; Yu, J. Q. *Nature* **2012**, *486*, 518.

(19) Cheng, C.; Hartwig, J. F. *Science* **2014**, *343*, 853.

(20) Rousseau, G.; Breit, B. *Angew. Chem., Int. Ed.* **2011**, *50*, 2450.

(21) Cornella, J.; Righi, M.; Larrosa, I. *Angew. Chem., Int. Ed.* **2011**, *50*, 9429.

(22) Chernyak, N.; Dudnik, A. S.; Huang, C. H.; Gevorgyan, V. *J. Am. Chem. Soc.* **2010**, *132*, 8270.

(23) Wang, C.; Chen, H.; Wang, Z.; Chen, J.; Huang, Y. *Angew. Chem., Int. Ed.* **2012**, *51*, 7242.

(24) Maehara, A.; Tsurugi, H.; Satoh, T.; Miura, M. *Org. Lett.* **2008**, *10*, 1159.

(25) Mochida, S.; Hirano, K.; Satoh, T.; Miura, M. *Org. Lett.* **2010**, *12*, 5776.

(26) Dydio, P.; Reek, J. N. H. *Chem. Sci.* **2014**, *5*, 2135.

(27) Kuhl, N.; Hopkinson, M. N.; Wencel-Delord, J.; Glorius, F. *Angew. Chem., Int. Ed.* **2012**, *51*, 10236.

(28) Sherry, A. E.; Wayland, B. B. *J. Am. Chem. Soc.* **1990**, *112*, 1259.

(29) Zhang, X. X.; Wayland, B. B. *J. Am. Chem. Soc.* **1994**, *116*, 7897.

(30) Nelson, A. P.; DiMagno, S. G. *J. Am. Chem. Soc.* **2000**, *122*, 8569.

(31) Colby, D. A.; Tsai, A. S.; Bergman, R. G.; Ellman, J. A. *Acc. Chem. Res.* **2012**, *45*, 814.

(32) Bouffard, J.; Itami, K. *Top. Curr. Chem.* **2010**, *292*, 231.

(33) Grushin, V. V.; Thorn, D. L.; Marshall, W. J.; Petrov, V. A. *Activation and Functionalization of C−H Bonds*; ACS Symposium Series 885; American Chemical Society: Washington, DC, 2004; p 393.

(34) Oxgaard, J.; Tenn, W. J.; Nielsen, R. J.; Periana, R. A.; Goddard, W. A. *Organometallics* **2007**, *26*, 1565.

(35) IES is also referred to as intramolecular proton transfer (IPT): Cundari, T. R.; Grimes, T. V.; Gunnoe, T. B. *J. Am. Chem. Soc.* **2007**, *129*, 13172.

(36) Lapointe, D.; Fagnou, K. *Chem. Lett.* **2010**, *39*, 1118.

(37) Grushin, V. V.; Marshall, W. J.; Thorn, D. L. *Adv. Synth. Catal.* **2001**, *343*, 161.

(38) Zakzeski, J.; Behn, A.; Head-Gordon, M.; Bell, A. T. *J. Am. Chem. Soc.* **2009**, *131*, 11098.

(39) Tan, R. Y.; Jia, P.; Rao, Y. L.; Jia, W. L.; Hadzovic, A.; Yu, Q.; Li, X.; Song, D. T. *Organometallics* **2008**, *27*, 6614.

(40) Zhao, S.-B.; Wang, S. *Chem. Soc. Rev.* **2010**, *39*, 3142.

(41) Willems, S. T. H.; Budzelaar, P. H. M.; Moonen, N. N. P.; de Gelder, R.; Smits, J. M. M.; Gal, A. W. *Chem.—Eur. J.* **2002**, *8*, 1310.

(42) Liu, Z. J.; Yamamichi, H.; Madrahimov, S. T.; Hartwig, J. F. *J. Am. Chem. Soc.* **2011**, *133*, 2772.

(43) Kanas, D. A.; Geier, S. J.; Vogels, C. M.; Decken, A.; Westcott, S. A. *Inorg. Chem.* **2008**, *47*, 8727.

(44) Geier, S. J.; Chapman, E. E.; McIsaac, D. I.; Vogels, C. M.; Decken, A.; Westcott, S. A. *Inorg. Chem. Commun.* **2006**, *9*, 788.

(45) Budzelaar, P. H. M.; Moonen, N. N. P.; de Gelder, R.; Smits, J. M. M.; Gal, A. W. *Chem.—Eur. J.* **2000**, *6*, 2740.

(46) Marsh, R. E. *Acta Crystallogr., Sect. B* **2004**, *60*, 252.

(47) Zakzeski, J.; Burton, S.; Behn, A.; Head-Gordon, M.; Bell, A. T. *Phys. Chem. Chem. Phys.* **2009**, *11*, 9903.

(48) Crabtree, R. H. *The organometallic chemistry of the transition metals*, 5th ed.; Wiley: Hoboken, NJ, 2009.

(49) While we were unable to successfully isolate complex **5**, DFT calculations predict the rate of H/D exchange to be faster with $\Delta H^{\ddagger}$ = 15.0 kcal/mol (298 K) and $\Delta G^{\ddagger}$ = 17.6 kcal/mol (298 K) (see Supporting Information).